J Opt
DOI 10.1007/s12596-013-0125-1

RESEARCH ARTICLE

Digital image dual watermarking using self-fractional fourier functions, bivariate empirical mode decomposition and error correcting code

J. B. Sharma · K. K. Sharma · Vineet Sahula

Received: 24 April 2012 / Accepted: 18 January 2013

Abstract In some legal, medical and military applications, image authentication is a mandatory requirement for copyright protection and security. In this paper, a novel dual (robust and fragile) watermarking scheme based on self-fractional Fourier functions and bivariate empirical mode decomposition with cyclic error correcting code is proposed. In this technique image is decomposed into M self-fractional Fourier function (SFFF) images, The SFFF images are further decomposed into intrinsic mode functions (IMFs) using bivariate empirical mode decomposition (BiEMD). Watermarks are encoded using cyclic error correction coding and embedded in the residue signal obtained by BiEMD of SFFF images. A procedure to generate a new type of fragile watermark called barmark is developed. Proposed scheme has the capability of self-authentication of the watermarked images along with robustness and security. The proposed decomposition technique provides flexibility in the number of watermarking bits that can be added (payload capacity) in a given image. Use of some transform before SFFF decomposition will provide additional degree of freedom in security and robustness. Robustness of recovery is improved by error correction coding of the watermarks. The proposed scheme can be used for complex images due to the use of bivariate EMD. Simulation results under different test conditions are presented to validate the efficacy of the proposed scheme.

Keywords Image watermarking · Empirical mode decomposition (EMD) · Fractional Fourier transform · Self-fractional Fourier transforms

J. B. Sharma (✉) · K. K. Sharma · V. Sahula
Department of Electronics & Communication Engineering,
Malaviya National Institute of Technology,
Jaipur, Rajasthan, India
e-mail: jballabh.sharma@gmail.com

K. K. Sharma
e-mail: kksharma_mrec@yahoo.com

V. Sahula
e-mail: vineetsahula@ieee.org

Introduction

With rapid growth of digital multimedia and internet technology, the issues related to the copyright violation, illegal distribution, forged authentication have become important. The prevention of piracy of digital multimedia objects has, therefore, been a major challenge [1]. Digital watermarking provides a solution to prove the ownership of digital data and to prevent illegal duplication, interpolation and distribution of multimedia data [1–6]. The watermarking algorithm should meet few basic requirements like imperceptibility, robustness, security and authentication, etc., [2–4].

A digital watermark is a secret imperceptible signal which is embedded into the original data in such a way

Published online: 16 March 2013

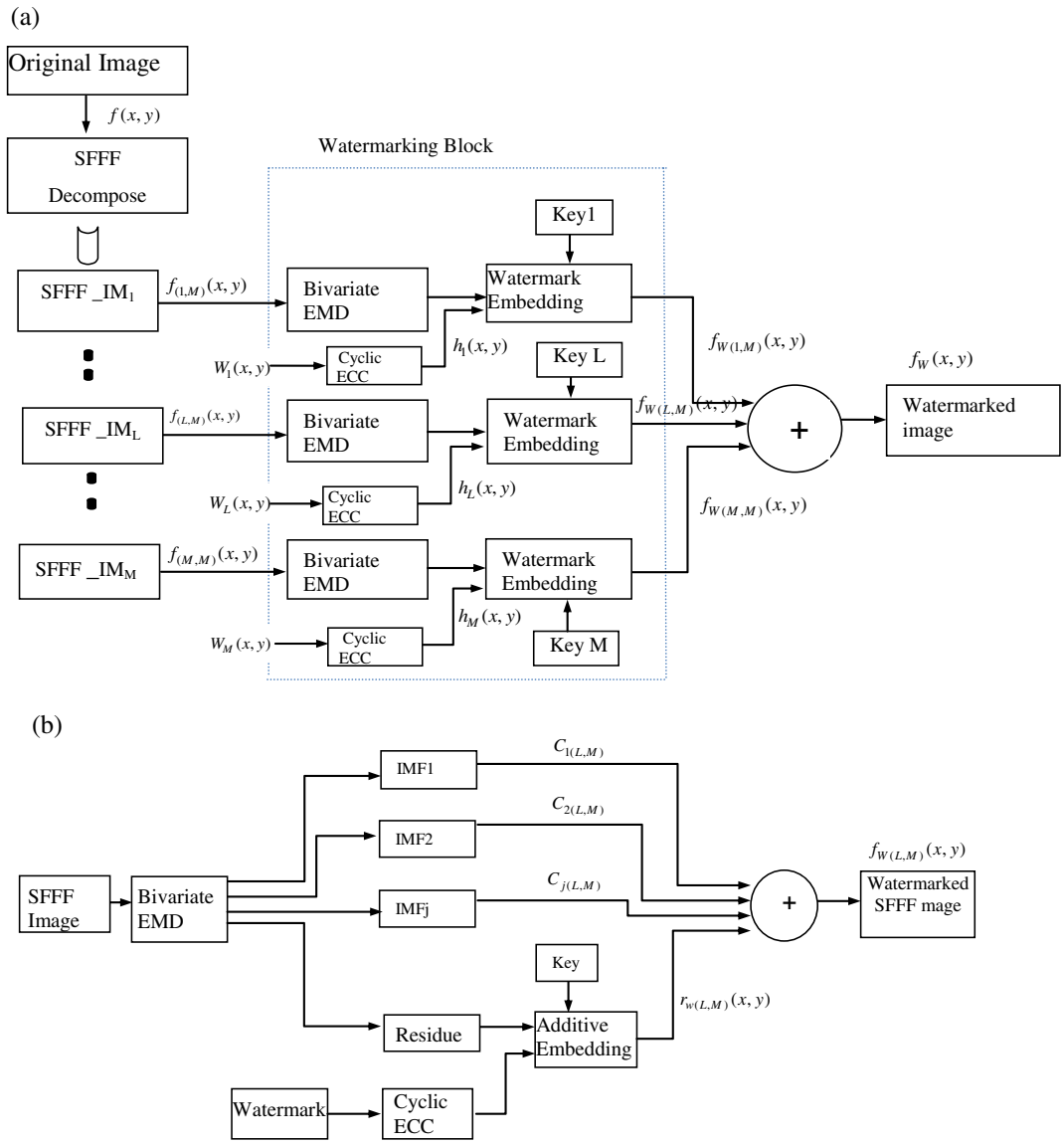

Fig. 1 **a** Block diagram of proposed watermarking scheme. **b** Watermarking block internal structure

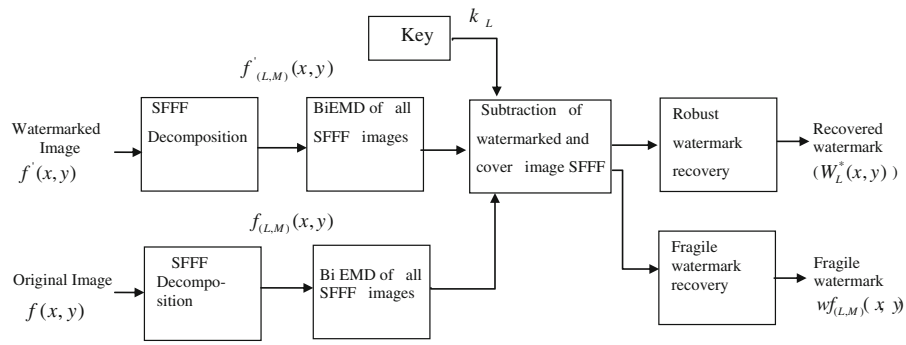

Fig. 2 Watermark detection process

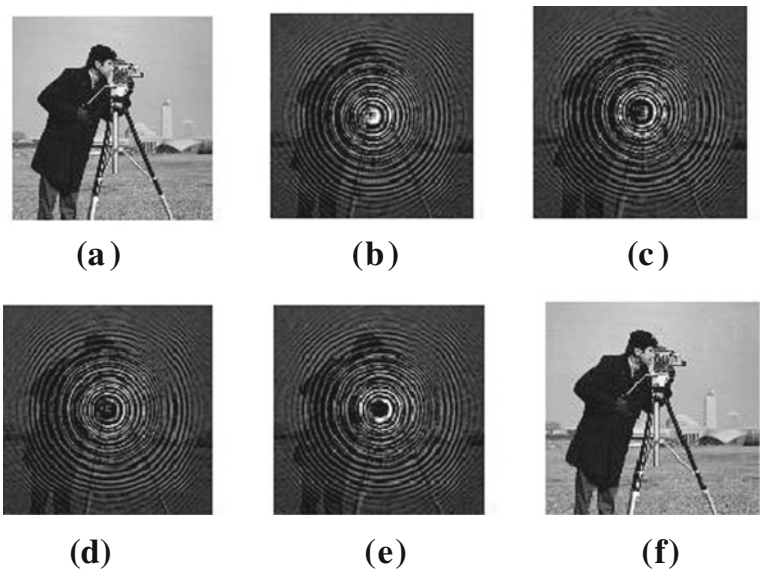

Fig. 3 **a** Cameraman image **f** Watermarked image **b**, **c**, **d**, **e** Water marked SFFF image

that it remains present as long as the perceptible quality of the content is at an acceptable level. The owner of the original data proves his/her ownership by extracting the watermark from the watermarked content in case of multiple ownership claims. Digital watermark can be classified as robust watermark, fragile watermark and semi-fragile watermark [4]. The robust watermark survives when the watermarked image is attacked and thus it is used for copyright protection. The fragile watermark changes slightly due to changes done in the watermarked image content. Because of this property, fragile watermarking is used for image authentication [7]. Semi-fragile watermarks provide a compromise between robustness and fragility. They are robust to "content preserving" operations (such as JPEG compression) and fragile to "content altering" transforms as reported in [8].

The watermarking schemes have been proposed in spatial domain [1, 2] as well as transform domains

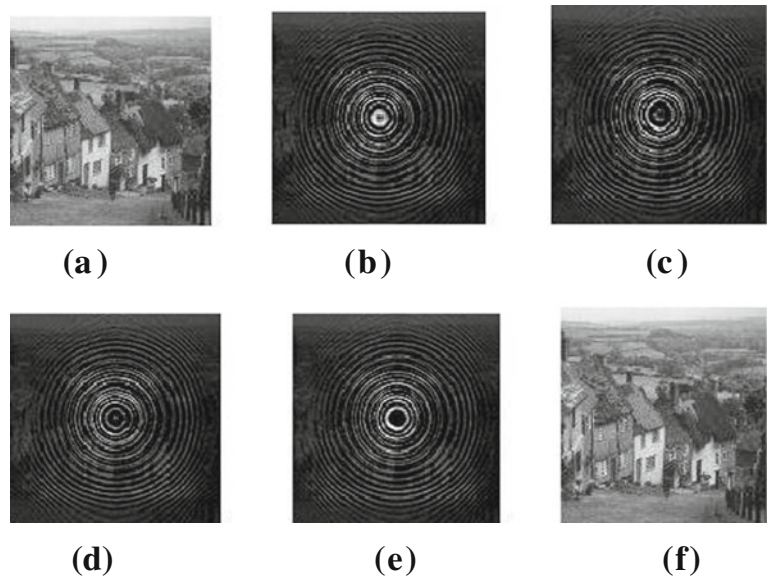

Fig. 4 **a** Goldhill image **f** Watermarked image **b**, **c**, **d**, **e** Watermarked SFFF images

[3–14], where the spatial and transform coefficients of the image are modified either in multiplicative manner or in additive manner. Transform domain watermarking techniques using discrete cosine transform (DCT) [3, 4], discrete wavelet transform (DWT) [6, 7] and Fractional Fourier transform (FrFT) [5] have been proposed, where the transform coefficients of the image are modified, to embed the watermark. A robust watermarking scheme based on decomposition of the host image using self fractional Fourier functions is proposed in [9]. Different robust watermarking schemes using empirical mode decomposition (EMD) have also been proposed in [10–14]. However, none of the existing methods employ SFFF decomposition combined with bivariate empirical mode decomposition (BiEMD). The use of BiEMD with SFFF improves the robustness and security.

In this paper a new robust and fragile dual watermarking technique based on bivariate empirical mode decomposition of complex self-fractional Fourier functions and cyclic error correction code is presented. A procedure to generate a new type of fragile watermark called barmark used for self authentication of image is also proposed. Fragile watermark is a function of original image, watermark being embedded, encoding scheme and number of SFFF components. This self generated fragile watermark can be used for image authentication.

Decomposition of image in self fractional Fourier function images before bivariate empirical mode decomposition provides flexibility to embed multiple watermarks and transform before SFFF decomposition. Encoding of watermark and encryption/decryption of key provide additional robustness and security. Self generated fragile watermark provides the ability to self authenticate the image.

The rest of the paper is organized as follows: In section II a review of fractional Fourier transform, self-fractional Fourier functions, bivariate empirical mode decomposition and cyclic error correcting coding is presented. Section III describes the proposed watermark embedding and detection strategy. Section IV gives the simulation results and the conclusions of work are given in section V.

Overview of FRFT, SFFF, EMD, bivariate EMD

Fractional Fourier transform

The fractional Fourier transform is the generalized verson of the Fourier transform. The α order fractional

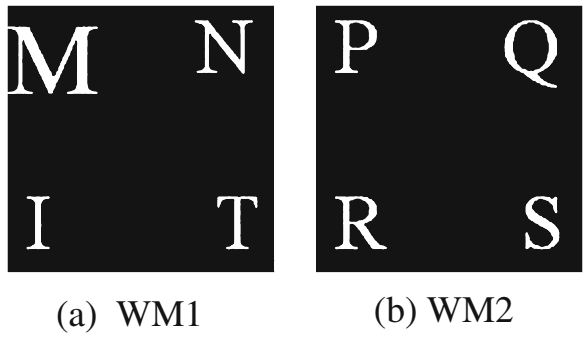

Fig. 5 Original watermarks

Fourier transform $F^{\alpha}(u)$ is defined as [15–20]:

$$\mathcal{F}^{\alpha}(u) = \int_{-\infty}^{\infty} f(x) K_{\alpha}(x,u)\,dx, \tag{1}$$

and

$$f(x) = \int_{-\infty}^{\infty} \mathcal{F}^{\alpha}(u) K_{\alpha}^{*}(x,u)\,dx\,, \tag{2}$$

where transform kernel $K_{\alpha}(x,u)$ of the FRFT is given by

$$K_{\alpha}(x,u) = \begin{cases} \sqrt{\frac{1-j\cot\alpha}{2\pi}}\, e^{j\left\{\frac{u^2+x^2}{2}\right\}\cot\alpha} e^{-jux\csc\alpha} \\ \text{if } \alpha \neq \mathrm{N}\pi, \ \ \mathrm{N} \text{ is integer} \\ \quad \delta(x-u), \ \ \text{if } \alpha = 2\mathrm{N}\pi, \ \mathrm{N} \text{ is integer} \\ \quad \delta(x+u), \ \ \text{if } \alpha = (2\mathrm{N}+1)\pi, \ \mathrm{N} \text{ is integer} \end{cases}$$

α is the rotation angle of the transformed signal in the wigner domain and the superscript * denotes complex conjugation. The FRFT reduces to the conventional FT when $\alpha=\pi/2$.

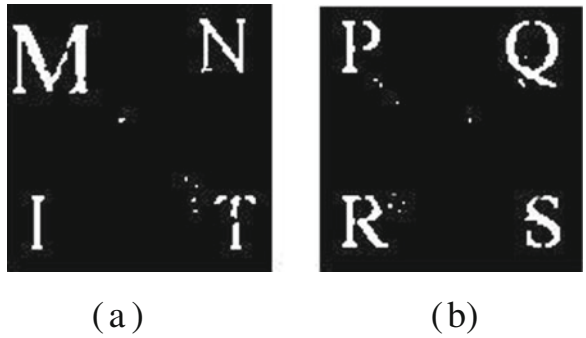

Fig. 6 Recovered watermark

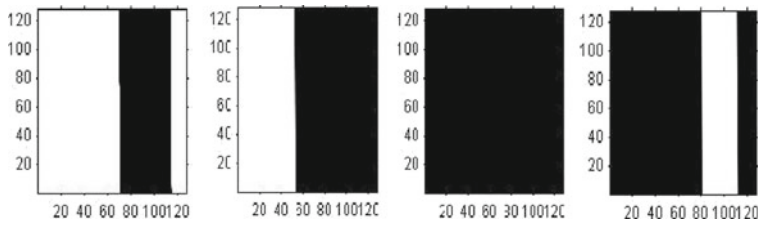

Fig. 7 a–d Barmarks of four SFFF components of Cameraman image with WM1 watermark

Self-fractional Fourier transform

Self-fractional Fourier function (SFFF) is a function, which is invariant under the fractional Fourier transformation for some angle α. A function from Hilbert space of finite energy signal can be represented as a sum of M SFFFs which are orthogonal to each other [17–20]. The self-fractional Fourier function (SFFF) $F(x)$ of rational order $\alpha=N/M$ is defined as [16, 17],

$$F(x)=\left[\mathsf{F}^{0}+\mathsf{F}^{(N/M)}+\ldots\ldots\mathsf{F}^{(k-1)N/M}\right]g(x), \tag{3}$$

where $g(x)$ be any generator function . We can represent $g(x)$ through the sum of M orthogonal SFFFs of order M as,

$$g(x)=\sum_{L=0}^{M-1}F(x)_{M,L}, \tag{4}$$

where

$$F(x)_{M,L}=\frac{1}{M}\sum_{k=1}^{M}\exp\left(\frac{i2\pi L(k-1)}{M}\right)R^{\frac{2\pi(k-1)}{M}}[g(u)](x) \tag{5}$$

$F(x)_{M,L}$ is a SFFF. Here k and L are the smallest integers that satisfy $kN/4L$ for the given N and M.

Empirical mode decomposition

Empirical mode decomposition proposed in [21] is a fully data driven, self-adaptive technique for decomposition of signal into oscillatory components called intrinsic mode functions (IMFs) and the coarsest component which is termed as mean trend or residue. In this method, a signal is projected onto basis functions which are directly derived from the data, instead of predefined basis functions [22]. The coarsest component of EMD based decomposed signal is highly robust for attacks like noise and JPEG compression [10, 14]. Using EMD, the input image $f(x,y)$ is decomposed as [21]:

$$f(x)=\sum_{j=1}^{n}C_j(x)+r(x), \tag{6}$$

where $C_j(x)$ are called Intrinsic Mode Functions, $r(x)$is residue or mean trend. The details of EMD algorithm to decompose a signal is available in [21] for ready reference.

Bivariate empirical mode decomposition

For complex signals a different approach for empirical mode decomposition is adopted. Bivariate EMD proposed by Gabriel Rilling et al. [23] is more general-

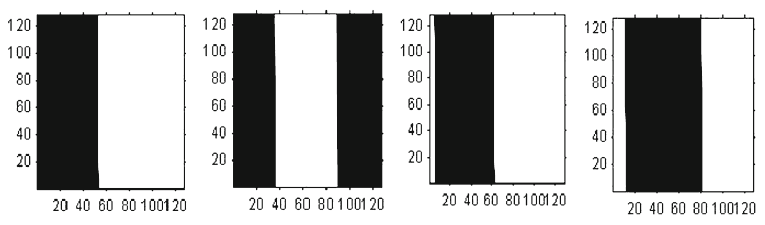

Fig. 8 a–d Barmark for Cameraman image withWM2 watermark

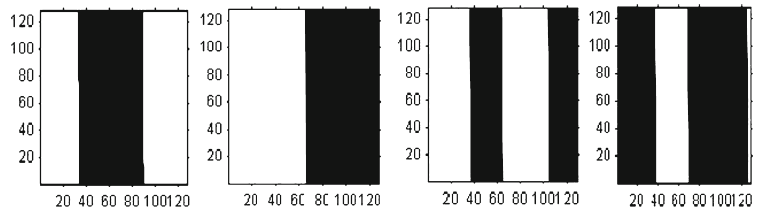

Fig. 9 a–d Barmark for Goldhill image with WM1 watermark

ized extension of EMD for complex domain [24]. The bivariate EMD algorithm is designed to extract zero mean rotating components. The zero mean rotating components are termed as complex valued/-bivariate IMFs. Rotating component IMFs make it more stable and generalized. Algorithm used for Bivariate EMD is available in [23].

Proposed watermarking scheme

The proposed watermarking scheme is based on decomposition of an image or its transformed version using SFFFs and BiEMD. This combination of SFFF with BiEMD offers increased robustness of the watermarking scheme.

Direct EMD is applied on image signal in the schemes proposed in [10–14], but in this scheme EMD is applied on SFFF decomposed complex images.

Error correction coding (ECC) is used to reduce the error added by the attacks on the watermark. Cyclic encoding provides flexibility to specify generator polynomial for encoding. Hence, cyclic encoding gives additional degree of freedom for watermark security with the error correction.

The original image $f(x,y)$ or its transformed version is decomposed into M SFFF images $f_{(L,M)}(x,y)$, L=1, 2…, M using (5).

$$f(x,y) = \sum_{L=1}^{M} f_{(L,M)}(x,y) \tag{7}$$

All the SFFF decomposed images $f_{(L,M)}(x,y)$ are further decomposed by BiEMD into IMFs $C_{j(L,M)}(x,y)$ and residue $r_{(L,M)}(x,y)$ signals using (5) .We has

$$f_{(L,M)}(x,y) = \sum_{j=1}^{n} C_{j(L,M)}(x,y) + r_{(L,M)}(x,y) \tag{8}$$

where L=1, 2, 3.....M, j=1, 2, 3.....n.

Watermark $w_L(x,y)$ is first encoded using cyclic error correcting coding, with generator polynomial as a row containing the coefficients in order of ascending powers.

Encoded watermark $h_L(x,y)$ is then added into residue signals $r_{(L,M)}(x,y)$ of each SFFF image according to respective key k_L.

Watermarked residue signal $r_{W(L,M)}(x,y)$ is obtained by adding watermark $h_L(x,y$ into residue signals $r_{(L,M)}(x,y)$ as follows:

$$r_{W(L,M)}(x,y) = r_{(L,M)}(x,y) + ah_L(x,y), \tag{9}$$

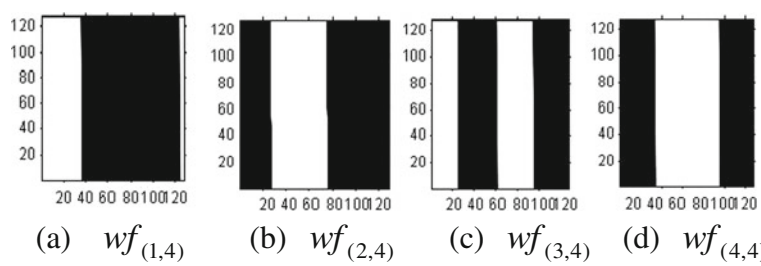

Fig. 10 a–d Barmark for Goldhill image with WM2 watermark

Table 1 Coordinates of black bars in fragile watermarks of images

Image	Cameraman				Goldhill			
	$wf_{(1,4)}(x,y)$	$wf_{(2,4)}(x,y)$	$wf_{(3,4)}(x,y)$	$wf_{(4,4)}(x,y)$	$wf_{(1,4)}(x,y)$	$wf_{(2,4)}(x,y)$	$wf_{(3,4)}(x,y)$	$wf_{(4,4)}(x,y)$
Watermark	First watermark WM1 using letters M, N, I, T				M, N, I, T			
No. of BARS	1	1	1	2	1	1	2	2
Column coordinates of start and end of Black BAR	69,114	51,128	(1,128)	(1,81) (111,128)	(32,90)	(65,128)	(38, 65), (106,108)	(1, 38) (70, 126)
Watermark	Second watermark WM2 using letters P, Q, R, S				P, Q, R, S			
No. of BARS	1	1	2	1	1	2	2	2
Column coordinates of start and end of Black BAR	(10,81)	(5,63)	(1,36) (89,128)	(1, 53)	(34, 124)	(1,27) (75,128)	(23,62) (93, 128)	(1, 34) (94, 128)

where scaling parameter a is multiplied to adjust the visibility and robustness against attacks.

The watermarked SFFF images $f_{W(L,M)}(x,y)$ are obtained by adding all the IMFs $C_{j(L,M)}(x,y)$ of (8) and the watermarked residue $r_{W(L,M)}(x,y)$ in (9) as follows

$$f_{W(L,M)}(x,y) = \sum_{j=1}^{n} C_{j(L,M)}(x,y) + r_{W(L,M)}(x,y). \quad (10)$$

The above scheme is shown in Fig. 1(a) and (b). The watermarked image $f_W(x,y)$ is reconstructed by adding watermarked SFFF images $f_{W(L,M)}(x,y)$,

$$f_W(x,y) = \sum_{L=1}^{M} f_{W(L,M)}(x,y), L = 1,2,..M. \quad (11)$$

The above procedure is summarized as follows:

Step 1: Decompose the original image into M SFFF images using Self-fractional Fourier functions using (7).

Step 2: Decompose each SFFF image into IMFs and residue using (8).

Step 3: Encode input watermarks $W_L(x,y)$ using systematic cyclic error correcting code to get encoded watermark $h_L(x,y)$ and generate key k_L.

Step 4: Embed the encoded watermark $h_L(x,y)$ in the residue $r_{(L,M)}(x,y)$ of the SFFF image using (9) and key k_L. Obtain watermarked SFFF image $f_{W(L,M)}(x,y)$ using (10).

Step 5: Find watermarked image $f_W(x,y)$ by adding all the watermarked SFFF images $f_{W(L,M)}(x,y)$ using (11).

Robust watermark detection and fragile watermark generation procedure

Detection of watermark is performed by repeating the process of decomposition of any test image $f'(x,y)$. Process of robust watermark detection and fragile watermark generation is shown in Fig. 2. $f'(x,y)$ is decomposed to obtain SFFF images $f'_{(L,M)}(x,y)$ and further into IMFs $C'_{j(L,M)}(x,y)$ and

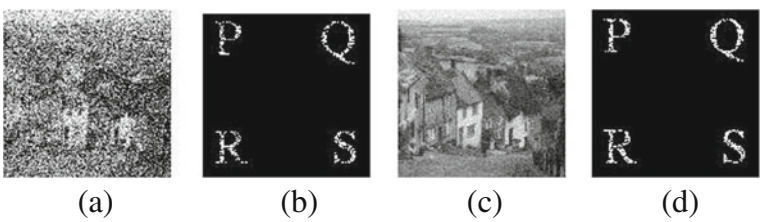

(a) (b) (c) (d)

Fig. 11 **a**, **b** Attacked image and recovered watermark with 25 dB SNR. **c** Attacked image **d** Recovered watermark with 40 dB SNR

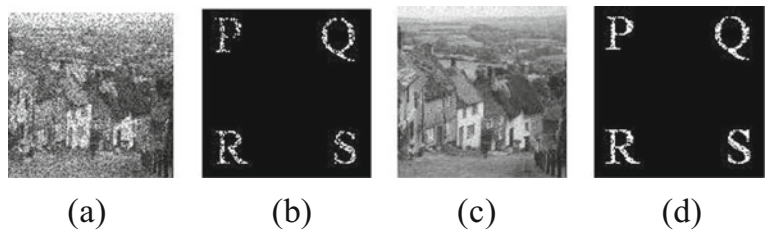

Fig. 12 **a**, **c** Attacked image **b**, **d** Recovered watermark with 25 dB and 40 dB SNR

residue $r'_{(L,M)}(x,y)$ using (5),and (6) as

$$f'(x,y) = \sum_{L=1}^{M} f'_{(L,M)}(x,y),\ L = 1,2,....M, \tag{12}$$

$$f'_{(L,M)}(x,y) = \sum_{j=1}^{n} C'_{j(L,M)}(x,y) + r'_{(L,M)}(x,y) \tag{13}$$

Robust watermark $W_L^*(x,y)$ is recovered by cyclic decoding of encoded robust watermark $h^*(x,y)$, where $h^*(x,y)$ is obtained by subtracting the original image IMFs $C_{j(L,M)}(x,y)$ from watermarked image IMFs $C'_{j(L,M)}(x,y)$, thereafter adding the difference values and considering scaling parameter a, as

$$\begin{aligned} ew_L &= \sum_{j=1}^{n} \left[C'_{j(L,M)}(x,y) - C_{j(L,M)}\right] \\ h_L^*(x,y) &= \tfrac{ew_L}{a}, \\ h^*(x,y) &= \sum_{L=1}^{M} h_L^*(x,y) \end{aligned} \tag{14}$$

The fragile watermark $wf_{(L,M)}(x,y)$ is obtained by subtracting $r'_{(L,M)}(x,y)$ from $r_{(L,M)}(x,y)$ as

$$wf_{(L,M)}(x,y) = r'_{(L,M)}(x,y) - r_{(L,M)}(x,y), \tag{15}$$

where L=1,2,3.....M.

It may be mentioned here that this watermark $wf_{(L,M)}(x,y)$ is dependent on $f(x,y)$, $h(x,y)$ and M.

Steps for robust watermark detection and fragile watermark generation are summarized as follows:

Step 1: Decompose the watermarked image using self fractional Fourier functions using (12) and obtain M SFFF watermarked SFFF images $f'_{(L,M)}(x,y)$.

Step 2: Decompose each watermarked SFFF image into its IMFs and residue using BiEMD decomposition using (13).

Step 3: Find encoded watermark $h_L^*(x,y)$ by using (14) with respective key k_L.

Step 4: Decode the $h_L^*(x,y)$ using cyclic decoding and recover the watermark $W_L^*(x,y)$.

Step 5: Repeat steps 2–4 to recover all watermark characters.

Fragile watermark generation By using step 1 and step 2 given above, obtain the components $C'_{j(L,M)} \times (x,y)$ and $r'_{(L,M)}(x,y)$. Find the difference between $r_{(L,M)}(x,y)$ and $r'_{(L,M)}(x,y)$, and obtain fragile watermark (barmark) $wf_{(L,M)}(x,y)$ using (15).

Attacks

The malicious manipulations performed on watermarked image either intended or unintended are known as attacks [22]. Watermarks used for copyright

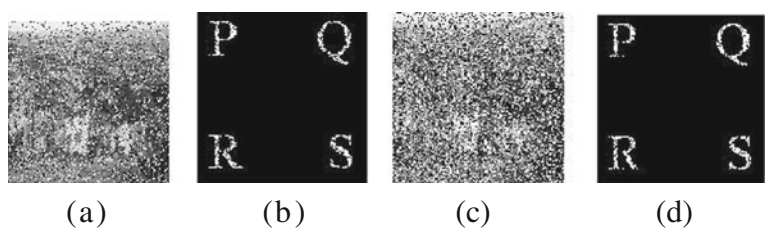

Fig. 13 **a**, **c** Attacked image **b**, **d** Recovered watermark with salt and pepper noise

Fig. 14 **a**, **c** Attacked image **b**, **d** Recovered watermark with Q=10,30

protection should therefore be robust against such attacks and it is one of the primary requirements of a watermarking schemes. We have performed the experiments to test the robustness of our watermarking scheme for image processing attacks, e.g., noise attacks (Gaussian, speckle, salt and pepper), filtering attacks (median, wiener, Gaussian), JPEG compression, image sharpening and Blurring.

Simulation result

In this section computer simulation results performed using MATLAB, to verify the proposed scheme, are presented. Cameraman and Goldhill images (Figs. 3(a) and 4(a)) with two sets of watermark characters, shown in Fig. 5(a) and (b) are used to verify the proposed algorithm. The value of M is taken as four.

The input watermarks are encoded by (9, 8) systematic cyclic error correction code. The cyclic encoding scheme and n=9 and k=8 is selected due to simplicity and convenience of implementation.

The image $f(x,y)$ is decomposed in four SFFF images ($f_{(1,4)}(x,y)$, $f_{(2,4)}(x,y)$, $f_{(3,4)}(x,y)$, $f_{(4,4)}(x,y)$) each SFFF image is watermarked using (10) and (11). Watermarked SFFF images ($f_{W(1,4)}(x,y)$, $f_{W(2,4)}(x,y)$, $f_{W(3,4)}(x,y)$, $f_{W(4,4)}(x,y)$) are shown in Figs. 3(b–e) and 4(b–e) and final watermarked images are $f_W(x,y)$ shown in Figs. 3(f) and 4(f). Value of embedding constant parameter 'a' is decided by experimentation to ensure invisibility and peak signal to noise ratio 42 dB, and a=0.00008 is selected.

Watermark is recovered by decomposing watermarked image $f_W(x,y)$ into SFFF images $f'_{(L,M)}(x,y)$ and SFFF images into IMFs $C'_{j(L,M)}(x,y)$ and residue $r'_{(L,M)}(x,y)$ as shown in Fig. 2. The recovered original watermarks are shown in Fig. 6(a–b).

Fragile watermark $wf_{(L,M)}(x,y)$ is generated by subtracting $r_{(L,M)}(x,y)$ from $r'_{(L,M)}(x,y)$.The fragile watermark barmarks $wr_{(L,M)}(x,y)$ are shown in Fig. 7(a–d) for Cameraman image with M, N, I, T character set in WM1 watermark. Figure 8(a–d) shows barmark for Cameraman image with P, Q, R, S character set in WM2 watermark.

Similar barmark results for Goldhill image with WM1 and WM2 watermarks are shown in Figs. 9(a–d) and 10(a–d).

The Start and end coordinates of barmark $wf_{(L,M)}(x,y)$ with the number of bars, for all combinations of original images and watermarks are presented in Table 1.

Fig. 15 **a** median filter attacked image **b** recovered watermark for 5×5 window

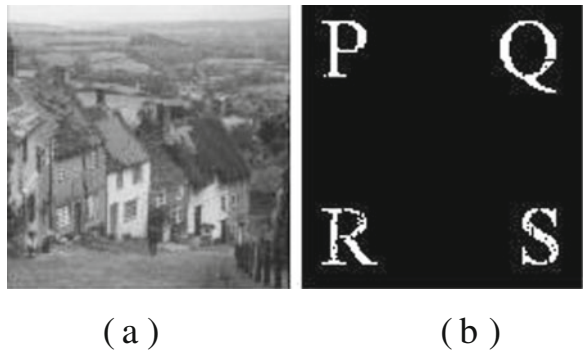

Fig. 16 **a** Gaussian filter attacked image **b** Recovered watermark for 5×5 window

(a) (b)

Fig. 17 **a** Wiener filter attacked image **b** Recovered watermark 5×5 window

It is evident that for given value of M, the barmark patterns $wf_{(L,M)}(x,y)$ are different for different combinations of watermarks and cover images. This pattern is unique and changes by changing image content.

Watermark detection with attacks

In this section simulation results for various image processing attacks including noise addition for different SNR, JPEG compression, filtering, sharpening, blurring, rotation to test the robustness of proposed scheme are presented.

Goldhill is used as cover image with WM2 (P,Q,R,S) watermark. First attack on the image is applied by adding white Gaussian noise with SNR 25 and 40 dB. Figure 11(a), (c) shows attacked images and Fig. 11 (b), (d) shows recovered watermarks for SNR of 25 dB and 40 dB respectively.

Speckle noise attack

Figure 12(a), (c) shows attacked image obtained by adding speckle noise of SNR 25 and 40 dB, Fig. 12(b), (d) shows recovered watermark.

(a) (b)

Fig. 18 **a** Attacked image **b** Recovered watermark

Salt and pepper noise

Figure 13(a), (c) shows attacked image obtained by mixing salt & pepper noise with sigma 0.2 and 0.4. Figure 13(b), (d) shows recovered watermark.

JPEG compression attack

Attacked image is obtained by applying JPEG compression with quality factor Q=10 and 30. Figure 14(a) shows attacked image and Fig. 14(b) shows recovered watermark.

Filter attack

Attacked image is obtained by applying median, Gaussian and wiener filtering with 5×5 window. Figures 15(a), 16 (a), and 17(a) represent attacked image and Figs. 15(b), 16 (b), and 17(b) represent recovered watermark.

Sharpening attack

Attacked image is obtained by applying 50 % sharpening of watermarked image. The attacked image is shown in Fig. 18(a) and recovered watermark in Fig. 18(b).

Blurring attack

Blur of linear motion of camera by 5 pixels, with an angle of 65° and 20 pixels, with an angle of 45 in a counterclockwise direction is applied to obtain attacked image. The attacked image is shown in Fig. 19(a), (c) and recovered watermark in Fig. 19(b), (d).

Rotation attack

Watermarked image is rotated between 2° and −2° to obtain attacked image . The attacked image is shown in Fig. 20(a), (c) and recovered watermark in Fig. 20 (b), (d) for rotation 2 and −2° respectively.

Comparison with other watermarking schemes and discussion

Proposed bivariate EMD combined with SFFF decomposition based implementation of robust watermarking is compared with watermarking scheme using only SFFF alone based decomposition and only bivariate EMD alone based decomposition. For this same

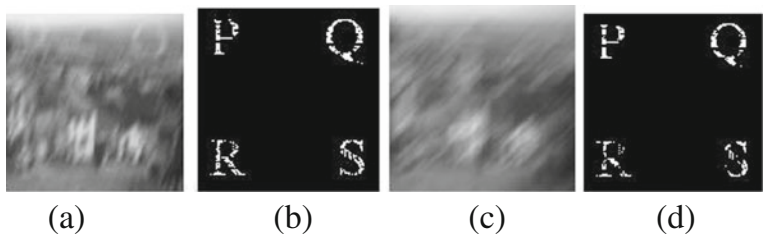

Fig. 19 **a**, **c** Attacked image **b**, **d** Recovered watermark

watermark encoded by systematic cyclic error correction code is embedded. Process used for embedding and detection in above two schemes is similar to proposed scheme.

Similarity (SIM) between extracted watermark $W^*(x,y)$ and original watermark $W(x,y)$ is used as performance parameter and defined as

$$SIM(W, W^*) = \frac{\sum_x \sum_y W(x,y).W^*(x,y)}{\sqrt{\sum_x \sum_y [W(x,y).W(x,y)]}\sqrt{\sum_x \sum_y [W^*(x,y).W^*(x,y)]}} \tag{16}$$

$W(x,y)$ = original watermark, $W^*(x,y)$ = Recovered watermark

Simulations are performed for above three schemes by embedding same watermark WM2 (P,Q,R,S) encoded by (9,8) cyclic error correcting code in goldhill image. Strength of embedded watermark is measured by peak signal to noise ratio (PSNR) of watermarked image, and is taken as 42 dB for applying attack on all three schemes.

Computation results of similarity parameter (SIM) defined in (16) for above three mentioned schemes, under different attacks, are presented in Tables 2 and 3. Figure 21(a), (b) represents the plot of similarity with respect to signal to noise ratio (SNR) of attacked image. Here SNR represent the signal to noise ratio of attacked image with respect to watermarked image.

Plot of similarity of extracted watermark for salt and pepper noise attack with respect to sigma of applied noise is shown in Fig. 22(a). Figure 22(b) shows the variation in similarity with respect to quality factor of JPEG compression attack.

It is clear from Tables 2 and 3 results of proposed scheme are superior in comparison to other two schemes in most of the attacks.

Proposed scheme is also having improved security due to two stage decomposition. A hacker cannot detect the watermark till the correct SFFF decomposition level (M) is not known. Other advantages include high robustness for robust watermark, secondly the fragile watermark for self authentication is developed for the proposed scheme only, which is also function of number of SFFF decomposition level (M).

Fig. 20 **a**, **c** Attacked image **b**, **d** Recovered watermark

Table 2 Similarity Index for Goldhill image with WM2 (P,Q,R,S) watermark PSNR(Peak Signal to Noise Ratio of watermarked image with respect to original image): 42 dB

Attack	Parameter	Watermarking scheme		
		SFFF + BiEMD	BiEMD alone	SFFF alone
JPEG	Q=5	0.8152	0.7784	0.7965
	Q=10	0.8360	0.8133	0.8204
	Q=20	0.8456	0.8259	0.8259
	Q=30	0.8757	0.8589	0.8589
	Q=40	0.8816	0.8597	0.8597
	Q=50	0.8904	0.8753	0.8753
Gaussian Noise	SNR=10 dB	0.7252	0.7044	0.7340
	SNR=25 dB	0.7549	0.7402	0.7401
	SNR=40 dB	0.8244	0.7834	0.8109
Speckle Noise	SNR=10 dB	0.6905	0.7234	0.6951
	SNR=25 dB	0.7034	0.7506	0.7366
	SNR=40 dB	0.8686	0.8376	0.8476
Salt & Pepper	Sigma=0.2	0.8936	0.8947	0.8760
	Sigma=0.5	0.8309	0.8562	0.8157
	Sigma=0.6	0.8220	0.8072	0.7948
Gaussian Filter	3×3	0.9590	0.9711	0.9373
	5×5	0.9590	0.9711	0.9373
	7×7	0.9590	0.9711	0.9373
MEDIAN	3×3	0.8760	0.8529	0.8529
	5×5	0.8204	0.8021	0.8021
	7×7	0.7981	0.7759	0.7759
weiner	3×3	0.8619	0.8298	0.8298
	5×5	0.8149	0.7948	0.7948
	7×7	0.8013	0.7701	0.7701
Sharpening	–	0.7893	0.7759	0.7784
Blur1(5/65)	–	0.8259	0.8037	0.8037
Blur1(20/45)	–	0.7608	0.7366	0.7366

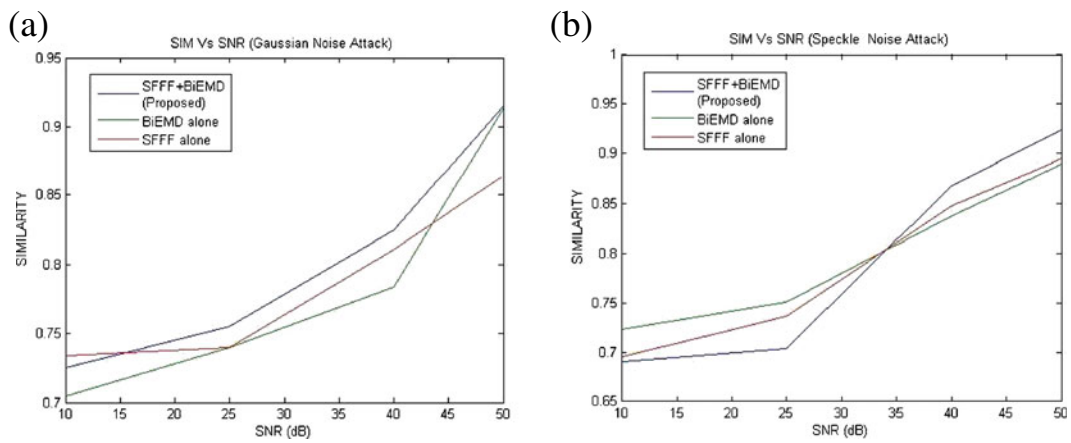

Fig. 21 Comparison of similarity (SIM) of extracted watermark after **a** Gaussian noise attack **b** speckle noise attack

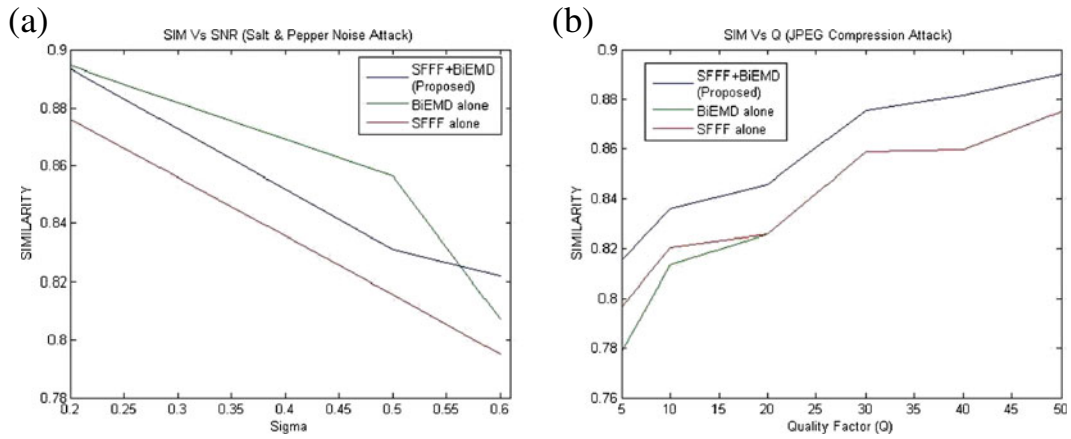

Fig. 22 Comparison of similarity (SIM) of extracted watermark after **a** salt & pepper noise attack **b** JPEG compression attack

Computation load of proposed scheme

Computation cost (load) of proposed scheme is the sum of the cost of SFFF computation and bivariate EMD computation. However, the computation cost for SFFF decomposition for NxN image size and M SFFF decomposition levels is $M{*}N^2 \log_2 N$, for more detail readers can refer [16, 17].

Bivariate decomposition computation cost is given as mentioned in [25]. Computational cost of the bivariate EMD is obtained by summing the complexity of computing a single IMF over the number of iterations (K_n) and the number of IMFs (J) as follows [25],

$$\sum_{n=1}^{J}\sum_{k=1}^{K_n} F\left(d_{n,k}\right),$$

where

$$F\left(d_{n,k+1}\right) = L(11P+2) + 15\sum_{p=1}^{P/2} M_R\left(d_{n,k,p}\right),$$

Where, J = Number of extracted IMFs, L = Data length, D = Data dimension, K_n = Number of shifting iteration to extract nth IMF , P = number of projections, $d_{n,k}$ = n-th IMF computed at the k-th iteration of the sifting process, $M_R(d_{n,k,p})$ = Number of extremas detected in the p-th projection of $d_{n,k}$, when P projection planes are used.

Since, Data length $L{=}NXN$, $P{=}4$ for our bivariate EMD algorithm, Hence $F\left(d_{n,k+1}\right) = 46(NXN) + 15\sum_{p=1}^{2} M_R\left(d_{n,k,p}\right)$, and $computation - load = \sum_{n=1}^{J}\sum_{k=1}^{K_n}[46(NXN) + 15\sum_{p=1}^{2} M_R(d_{n,k,p})]$

Table 3 Rotation Attack: SIMILARITY INDEX (SIM) (PSNR=42 dB)

Scheme	Angle (degrees)					
	−2°	−1°	−0.5°	0.5°	1°	2°
SFFF + BIEMD	0.7162	0.7034	0.7053	0.6905	0.6942	0.6810
BIEMD alone	0.7162	0.7034	0.7053	0.6905	0.6942	0.6810
SFFF alone	0.7162	0.7034	0.7053	0.6905	0.6942	0.6810

Conclusion

In this paper we have presented a new watermarking scheme with procedure to generate digital fragile barcode watermark (barmark) for self authentication of watermarked image. The importance of this scheme is that, it provides the solution to copy right protection, security and authentication. Due to use of BiEMD, it can be used for complex images (satellite and SAR images). The multistage decomposition added the possibility of encryption/decryption for security of watermark. The robustness and security is further improved by cyclic error correction encoding of the watermark. Simulation results have shown its robustness against attacks. On comparison with the only SFFF alone based and only BiEMD alone based schemes, results of proposed (SFFF combined with BiEMD) scheme are encouraging. More cost of computation is the disadvantage of this scheme.

References

1. I. Pits, A method for signature casting on digital images. Proc. IEEE Conf. Image Process., 215–218 (1996)
2. I.J. Cox, M.L. Miller, A.L. McKellips, Watermarking as communications with side information. Proc. IEEE **7**(87), 1127–1141 (1999)
3. C.C. Wai, DCT-based image watermarking using subsampling. IEEE Trans. Multimedia **5**(1), 34–38 (2003)
4. M. Habib, S. Sarhan, L. Rajab, A robust-fragile dual watermarking system in the DCT domain. Knowledge-Based Intelligent Information and Engineering Systems, Lecture Notes in Computer Science, 3682 (2005)
5. I. Djurovic, S. Stankovic, I. Pitas, Digital watermarking in the fractional Fourier transform domain. J. Netw. Comput. Appl. **24**(4), 167–173 (2001)
6. M. Barni, F. Bartiloni, A. Piva, Improved wavelet based watermarking through pixel wise masking. IEEE Trans. Image Process. **10**, 783–791 (2001)
7. A. Bohra, O. Farooq, Izharuddin, Blind self-authentication of images for robust watermarking using integer wavelet transform. Int. J. Electron. Commun. (AEÜ) **63**, 703–707 (2009)
8. E.T. Lina, C.I. Podilchukb, E.J. Delp, Detection of image alterations using semi-fragile watermarks. Proceedings of the SPIE International Conference on Security and Watermarking of Multimedia Contents II, 3971 (2000)
9. K.K. Sharma, D. Kumar Fageria, Watermarking based on image decomposition using self-fractional Fourier functions. J. Opt. **2**(40), 45–50 (2011)
10. N. Bi, Q. Sun, D. Huang, Z. Yang, J. Huang, Robust image watermarking based on multiband wavelets and empirical mode decomposition. IEEE Trans. Image Process. **8**(16), 1956–1996 (2007)
11. J. Taghia, M.A. Doostari, J. Taghia, An image watermarking method based on bidimensional empirical mode decomposition. Congr. Image Signal Process. **5**, 674–678 (2008)
12. A. Benkuider, A. Aarab, An Improved Watermarking Scheme Images based on the FABEMD. ICGST Int. J. Graph. Vis. Image Process. **11**, 9–17 (2011)
13. A. Sabri, M. Karoud, H. Tairi, A. Aarab, A. Robust, Image watermarking based on the empirical mode decomposition. Rev. Lit. Arts Am. **4**, 360–366 (2009)
14. Y. Lee, J. Nah, J. Kim, Digital image watermarking using bidimensional empirical mode decomposition in wavelet domain. IEEE International Symposium on Multimedia (2009)
15. C. Candan, M.A. Kutay, H.M. Ozaktas, The discrete fractional Fourier transform. IEEE Trans. Sig. Proc. **48**, 1329–1337 (2000)
16. H.M. Ozaktas, Z. Zalevsky, M.A. Kutay, *The fractional Fourier transform* (Wiley, Chichester, 2001)
17. T. Alieva, A.M. Barbe, Self-fractional Fourier functions and selection of modes. J. Phys. A: Math. Gen. **30**, L211–L215 (1997)
18. M.J. Coala, Self-Fourier functions. J. Phys. A: Math. Gen. **24**, L1143 (1991)
19. G. Cincotti, F. Gori, M. Santarsiero, Generalised self Fourier functions. J. Phys. A: Math. Gen. 25, (1992)
20. T. Alieva, On the self-fractional Fourier functions. J. PhysA: Math. Gen. **29**, L377–L379 (1996)
21. N.E. Huang, Z. Shen, S.R. Long, M.C. Wu, H.H. Shih, Q. Zheng, N.-C. Yen, C.C. Tung, H.H. Liu, The empirical mode decomposition and the Hilbert spectrum for nonlinear and non-stationary time series analysis. Proc. R. Soc. Lond. A **454**, 903–995 (1998)
22. A.P. Petitcolas, Watermarking schemes evaluation. IEEE Sig. Process. Mag. **5**(17), 58–64 (2000)
23. G. Rilling, P. Flandrin, P. Goncalves, J.M. Lilly, Bivariate empirical mode decomposition. IEEE Sig. Process. Lett. **14**, 936–939 (2007)
24. N. Rehman1, D. Looney,T. M. Rutkowski, D. P. Mandic, Bivariate EMD based image fusion. IEEE 15th workshop on statistical Signal Processing, 1626–1630 (2009)
25. J. Fleureau, A. Kachenoura, L. Albera, J.-C. Nunes, L. Senhadji, Multivariate empirical mode decomposition and application to multichannel filtering. Signal Process. **91** (12), 2783–2792 (2011)